

# NASA Technical Memorandum 85680

NASA-TM-85680 19840002843

## FIELD-INCIDENCE TRANSMISSION OF TREATED ORTHOTROPIC AND LAMINATED COMPOSITE PANELS

FOR REFERENCE

NOT TO BE TAKEN FROM THIS ROOM

LESLIE R. KOVAL

AUGUST 1983

LIBRARY COPY

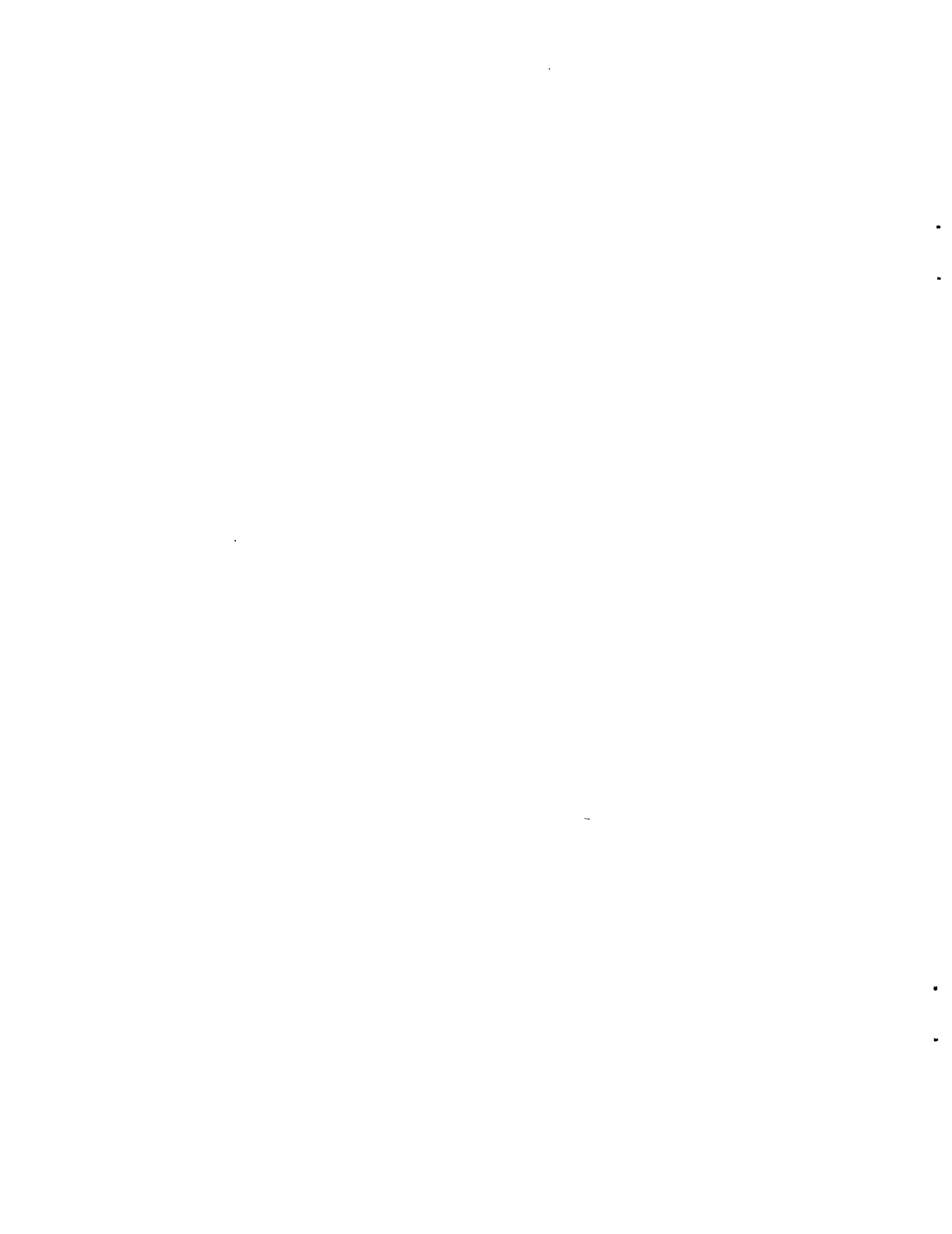
1983

LANGLEY RESEARCH CENTER  
LIBRARY, NASA  
HAMPTON, VIRGINIA



National Aeronautics and  
Space Administration

Langley Research Center  
Hampton, Virginia 23665



## INTRODUCTION

The pressures of rapidly escalating fuel costs have renewed interest in turboprop aircraft because of their higher propulsive efficiency. However, the high noise levels associated with the propeller at the blade passage frequency and its harmonics has generated concern about the acceptability of such aircraft and the weight penalties associated with interior noise control. This, in turn, has led to the requirement for a better understanding of the phenomenon of noise transmission through the sidewalls of the fuselage. In this spirit, the following is an analysis of the field-incidence transmission loss of infinite orthotropic and laminated composite panels which are treated by the use of various layers of noise insulation. The excitation is a plane wave incident at an oblique angle. Mixson, et al.<sup>1</sup>, have shown that this may be a satisfactory first-order approximation to the noise input from a propeller. Additionally, the effects of forward speed are also included. To make this analysis self-contained, sound propagation is analyzed from first principles, except for the equations used to model the fiberglass insulating blanket. These are taken from the appropriate papers by Beranek.<sup>2,3</sup>

## LIST OF SYMBOLS

|                    |                                     |
|--------------------|-------------------------------------|
| $c$                | propagation speed                   |
| $d_A$              | depth of air gap                    |
| $d_B$              | depth of blanket                    |
| $D_x, D_{xy}, D_y$ | orthotropic bending stiffnesses     |
| $D_{ij}$           | composite plate bending stiffnesses |

LIST OF SYMBOLS (cont.)

|                         |  |
|-------------------------|--|
| f                       | frequency, Hz                          |
| j                       | $\sqrt{-1}$                            |
| k                       | structure factor of blanket            |
| $k_{ix}, k_{iy}, \dots$ | wave numbers in the ith layers         |
| K                       | compressibility of air in blanket      |
| $m_p$                   | mass/area of panel                     |
| $m_t$                   | mass/area of septum or trim panel      |
| $M_1$                   | Mach number of external flow           |
| p                       | sound pressure                         |
| P                       | pressure amplitude                     |
| $R_1$                   | flow resistivity of blanket            |
| t                       | time                                   |
| u                       | media particle velocity                |
| V                       | external flow velocity                 |
| w                       | panel displacement                     |
| W                       | panel displacement amplitude           |
| x,y,z                   | coordinates                            |
| Y                       | porosity of blanket                    |
| Z                       | impedance                              |
| $\eta$                  | loss factor of panel                   |
| $\theta$                | incidence angle (measured from normal) |
| $\rho_0$                | density of air in blanket              |
| $\rho_m$                | bulk density of blanket                |
| $\omega = 2\pi f$       | circular frequency                     |

## MATHEMATICAL MODEL

For the sake of a specific example, attention is first given to an infinite orthotropic panel having a multi-layered treatment consisting of an airgap, a fiberglass blanket, and a septum (see fig. 1). Relative to the coordinate system shown, the incident plane wave is inclined at angle  $\theta$ , to the normal, and makes an angle  $\phi$  to the x axis. The airgap has a depth  $d_2$  and the blanket a thickness  $d_3$ . Other symbols are defined in a separate List of Symbols included in this report.

The equations for each of the layers are as follows:

Panel:

$$D_x \frac{\partial^4 w}{\partial x^4} + 2 D_{xy} \frac{\partial^4 w}{\partial x^2 \partial y^2} + D_y \frac{\partial^4 w}{\partial y^4} + m_p \frac{\partial^2 w}{\partial t^2} = (p_i + p_r - p_2)_{z=0} \quad (1)$$

Airgap:

$$\frac{\partial^2 p_2}{\partial x^2} + \frac{\partial^2 p_2}{\partial y^2} + \frac{\partial^2 p_2}{\partial z^2} = \frac{1}{c_2^2} \frac{\partial^2 p_2}{\partial t^2} \quad (2)$$

Blanket:

$$\frac{\partial^2 p_3}{\partial x^2} + \frac{\partial^2 p_3}{\partial y^2} + \frac{\partial^2 p_3}{\partial z^2} = \frac{\rho_0 k Y}{K} \frac{\partial^2 p_3}{\partial t^2} + \frac{R_1 Y}{K} \frac{\partial p_3}{\partial t} \quad (3)$$

Septum:

$$m_t \frac{\partial^2 w}{\partial t^2} = (p_3 + p_{3r} - p_4)_{z=d_2+d_3} \quad (4)$$

Interior:

$$\frac{\partial^2 p_4}{\partial x^2} + \frac{\partial^2 p_4}{\partial y^2} + \frac{\partial^2 p_4}{\partial z^2} = \frac{1}{c_4^2} \frac{\partial^2 p_4}{\partial t^2} \quad (5)$$

Equation (3) is consistent with the model formulated by Beranek<sup>2,3</sup> and is derived in Appendix A.

The incident plane wave is taken in the form

$$p_i = P_i \exp[j(\omega t - k_{ix} x - k_{iy} y - k_{iz} z)] \quad (6)$$

and the reflected wave is

$$p_r = P_r \exp[j(\omega t - k_{ix} x - k_{iy} y + k_{iz} z)] \quad (7)$$

The corresponding solutions to equations (1)-(5) are then:

Panel:

$$w_p = W_p \exp[j(\omega t - k_{px} x - k_{py} y)] \quad (8)$$

Airgap:

$$p_{2i} = P_2 \exp[j(\omega t - k_{2x} x - k_{2y} y - k_{2z} z)] \quad (9)$$

$$p_{2r} = P_{2r} \exp[j(\omega t - k_{2x} x - k_{2y} y + k_{2z} z)] \quad (10)$$

Blanket:

$$p_{3i} = P_3 \exp[j(\omega t - k_{3x} x - k_{3y} y)] e^{-k_3 \bar{z}} \quad (11)$$

$$p_{3r} = P_{3r} \exp[j(\omega t - k_{3x} x - k_{3y} y)] e^{k_3 \bar{z}} \quad (12)$$

where

$$\bar{z} = d - z = d_2 + d_3 - z$$

Septum:

$$w_z = W_z \exp [j(\omega t - k_{zx} x - k_{zy} y)] \quad (13)$$

Interior:

$$p_4 = P_4 \exp [j(\omega t - k_{4x} x - k_{4y} y + k_{4z}(z-d))] \quad (14)$$

In equations (6) and (7),

$$\begin{aligned} k_{1x} &= k_1 \sin \theta_1 \cos \phi \\ k_{1y} &= k_1 \sin \theta_1 \sin \phi \\ k_{1z} &= k_1 \cos \theta_1 \end{aligned} \quad (15)$$

where, via the convected wave equation,

$$k_i = (\omega/c_i) / (1 + M_1 \sin \theta_1 \cos \phi) \quad (16)$$

and  $M_1$  is the Mach number of the external flow (in the positive x-direction).

Matching trace wavelengths requires that

$$\begin{aligned} k_{px} = k_{2x} = k_{3x} = k_{4x} = k_{1x} &= k_1 \sin \theta_1 \cos \phi \\ k_{py} = k_{2y} = k_{3y} = k_{4y} = k_{1y} &= k_1 \sin \theta_1 \sin \phi \end{aligned} \quad (17)$$

and if

$$\begin{aligned} k_{ix} &= k_i \sin \theta_i \cos \phi \\ k_{iy} &= k_i \sin \theta_i \sin \phi, \quad i = 2, 3, 4 \end{aligned} \quad (18)$$

then

$$k_i \sin \theta_i = k_1 \sin \theta_1 \quad (19)$$

or

$$\sin \theta_i = (c_i / c) \sin \theta_1 / (1 + M_1 \sin \theta_1 \cos \phi) \quad (19a)$$

where  $k_i = \omega / c_i$ .

Equation (19a) gives the angles (to the normal) that the wave makes in each layer.

Further, satisfaction of the wave equation, equations (2) and (5), also requires that

$$k_{ix}^2 + k_{iy}^2 + k_{iz}^2 = k_i^2 = (\omega / c_i)^2 \quad (20)$$

or

$$k_{iz} = k_i \cos \theta_i, \quad i = 1, 2, \text{ or } 4 \quad (20a)$$

For the blanket, equation (3) requires that

$$b_3^2 = b^2 + k_{3x}^2 + k_{3y}^2 \quad (21)$$

or

$$b_3 = \sqrt{b^2 + (\omega / c_1)^2 \sin^2 \theta_1} \quad (21a)$$

where  $b$  is Beranek's complex propagation constant (see Appendix A, eq. (A-6)) for a flexible acoustical blanket.

The analysis is started by considering the trim panel first. Writing a force balance across the trim panel gives



$$-\omega^2 m_t w_t = (P_{3i} + P_{3r} - P_4)d \quad (22)$$

where  $d = d_2 + d_3$ .

Matching velocities at the interfaces between blanket, trim panel, and interior gives

$$(U_{3i} + U_{3r})_{z=0} = j\omega w_t = (U_4)_{z=d} \quad (23)$$

Now, the particle velocities "in the blanket" are related to the pressures by

$$U_{3i} = P_{3i}/Z_A, \quad U_{3r} = -P_{3r}/Z_A \quad (24)$$

where

$$Z_A = -j \left( \frac{K b_3}{\omega Y} \right)^* \quad (25)$$

is the characteristic impedance of the blanket. Similarly, for the interior,

$$U_4 = (k_{4z}/\rho_4 \omega) P_4 \quad (26)$$

From equations (26) and (23),

$$P_4 = j \left( \rho_4 \omega^2 / k_{4z} \right) W_t \quad (27)$$

Substituting  $P_4$  into equation (22),

$$P_{3i} + P_{3r} = j\omega Z_3 W_t \quad (28)$$

---

\*See Appendix B

where

$$\begin{aligned}
 Z_3 &= Z_t + Z_4 \\
 Z_t &= j\omega m_t \\
 Z_4 &= \rho_4 \omega^2 / k_{4z} = \rho_4 c_4 / \cos \theta_4.
 \end{aligned}
 \tag{29}$$

$Z_3$  is the input impedance into the trim panel (also the terminal impedance for the blanket),  $Z_t$  is the impedance of the trim panel (assumed here to be a septum), and  $Z_4$  is the input impedance into the interior.

One can also write, from equation (23),

$$(P_{3i} - P_{3r}) / Z_A = j\omega W_t \tag{30}$$

or,

$$P_{3i} - P_{3r} = j\omega W_t Z_A \tag{31}$$

From equations (28) and (31),

$$\begin{aligned}
 P_{3i} &= \frac{1}{2} (Z_3 + Z_A) j\omega W_t \\
 P_{3r} &= \frac{1}{2} (Z_3 - Z_A) j\omega W_t
 \end{aligned}
 \tag{32}$$

Next, pressures are to be matched at the airgap-blanket interface,

$$P_2 \Big|_{z=d_2} = P_3 \Big|_{z=d_3} \tag{33}$$

or

$$P_{2i} e^{-jk_{2z}d_2} + P_{2r} e^{jk_{2z}d_2} = P_{3i} e^{-k_3 d_3} + P_{3r} e^{k_3 d_3} \tag{34}$$

Matching velocities at the airgap-blanket interface,

$$U_{2i} e^{-jk_{2z}d_2} + U_{2r} e^{jk_{2z}d_2} = U_{3i} e^{-b_3d_3} + U_{3r} e^{b_3d_3} \quad (35)$$

The velocities and pressures in the airgap are related by

$$\rho_2 \frac{\partial u_2}{\partial t} = - \frac{\partial p_2}{\partial z} \quad (36)$$

which gives

$$U_{2i} = (k_{2z}/\rho_2 \omega) P_{2i} , \quad U_{2r} = -(k_{2z}/\rho_2 \omega) P_{2r} \quad (37)$$

Substituting equations (37) and (24) into (35) gives

$$P_{2i} e^{-jk_{2z}d_2} - P_{2r} e^{jk_{2z}d_2} = Z_R (P_{3i} e^{-b_3d_3} + P_{3r} e^{b_3d_3}) \quad (38)$$

where

$$Z_R = \rho_2 \omega / k_{2z} Z_A \quad (39)$$

Solving for  $P_{2i}$  and  $P_{2r}$  from equations (38) and (34)

$$2 P_{2i} e^{-jk_{2z}d_2} = (1+Z_R) P_{3i} e^{-b_3d_3} + (1-Z_R) P_{3r} e^{b_3d_3} \quad (40)$$

$$2 P_{2r} e^{jk_{2z}d_2} = (1-Z_R) P_{3i} e^{-b_3d_3} + (1+Z_R) P_{3r} e^{b_3d_3}$$

Taking the ratio,

$$\frac{P_{2r}}{P_{2i}} = R_2 e^{-j2k_{2z}d_2} \quad (41)$$

where

$$R_2 = \frac{(1-z_R) P_{3i} e^{-k_3 d_3} + (1+z_R) P_{3r} e^{k_3 d_3}}{(1+z_R) P_{3i} e^{-k_3 d_3} + (1-z_R) P_{3r} e^{k_3 d_3}} \quad (42)$$

Substituting for  $P_{3i}$  and  $P_{3r}$  via equation (32), it can be shown that  $R_2$  can be recast into the form (see Appendix C for details)

$$R_2 = \left(1 - \frac{P_2 \omega}{k_{23} Z_B}\right) / \left(1 + \frac{P_2 \omega}{k_{23} Z_B}\right) \quad (43)$$

where

$$\begin{aligned} Z_B &= Z_A \coth(k_3 d_3 + \psi_B) \\ &= \text{input impedance into the blanket} \\ \psi_B &= \coth^{-1}(Z_3/Z_A) \end{aligned} \quad (44)$$

Equation (41) can be rewritten as

$$P_{2r} = R_2 P_{2i} e^{-j 2 k_{23} d_2} \quad (45)$$

Now, attention is shifted to the panel. Writing a force balance across an element of the panel gives (via equation (1)),

$$j \omega Z_p W_p = P_i + P_r + (P_{2i} + P_{2r})_z = 0 \quad (46)$$

where  $Z_p$  is the impedance of the panel and is given by

$$Z_p = j \omega m_p \left[ 1 - (1+j\eta) \frac{D_x k_{px}^4 + 2D_{xy} k_{px}^2 k_{py}^2 + D_y k_{py}^4}{m_p \omega^2} \right] \quad (47)$$

where  $\eta$  is the loss factor of the panel.

Matching velocities at the panel-airgap interface gives

$$U_{2i} + U_{2r} = j \omega W_p \quad (48)$$

Substituting for velocities via equation (37),

$$P_{2i} - P_{2r} = j(\rho_2 \omega^2 / k_{23}) W_P \quad (49)$$

and using equation (45) in (48),

$$P_{2i} = \frac{j(\rho_2 \omega^2 / k_{23})}{1 - R_2 e^{-j 2 k_{23} d_2}} W_P \quad (50)$$

and

$$P_{2r} = j \left( \frac{\rho_2 \omega^2}{k_{23}} \right) \frac{R_2 e^{-j 2 k_{23} d_2}}{1 - R_2 e^{j 2 k_{23} d_2}} \quad (51)$$

so that

$$P_{2i} + P_{2r} = j \left( \frac{\rho_2 \omega^2}{k_{23}} \right) \frac{1 + R_2 e^{-j 2 k_{23} d_2}}{1 - R_2 e^{j 2 k_{23} d_2}} \quad (52)$$

After substituting for  $R_2$  via equation (43), it can be shown that

$$P_{2i} + P_{2r} = j \omega W_P Z_1 \quad (53)$$

where

$$Z_1 = (\rho_2 \omega / k_{23}) \coth(j k_{23} d_2 + \psi_2) \\ = \text{input impedance to airgap} \quad (54)$$

$$\psi_2 = \coth^{-1}(k_{23} Z_2 / \rho_2 \omega) \quad (55)$$

$Z_2 =$  terminal impedance of airgap  
 $= Z_B$  (for this problem)

Combining equation (53) with (46),

$$j\omega W_p Z_p^* = P_i + P_r \quad (56)$$

where

$$\begin{aligned} Z_p^* &= Z_p + Z_1 \\ &= \text{input impedance to panel} \end{aligned} \quad (57)$$

Finally, it remains to match displacements at the exterior surface of the panel. Letting  $\xi_1$  be the acoustic particle displacement in the external flowing media, then

$$\left(\frac{\partial}{\partial t} + V\frac{\partial}{\partial x}\right)^2 \xi_1 \Big|_{z=0} = -\frac{1}{\rho_1} \frac{\partial p}{\partial z} \Big|_{z=0} \quad (58)$$

where  $p = p_i + p_r$ . Taking  $\xi_1 = \xi_{10} \exp j(\omega t - k_{1x}x - k_{1y}y - k_{1z}z)$  gives

$$\xi_{10} = -j k_{1z} (P_i - P_r) / \rho_1 (\omega - V k_{1x})^2 \quad (59)$$

Matching displacements at the exterior surface of the panel requires that  $W_p = \xi_{10}$ , so that

$$W_p = -j k_{1z} (P_i - P_r) / \rho_1 (\omega - V k_{1x})^2 \quad (60)$$

Substituting for  $k_{1z}$  and  $k_{1x}$ ,

$$W_P = \frac{\cos \theta_1 (1 + M_1 \sin \theta_1 \cos \phi)}{j \rho_1 c_1 \omega} (P_i - P_r) \quad (61)$$

or

$$P_r = P_i - \frac{(j \omega W_P) \rho_1 c_1}{\cos \theta_1 (1 + M_1 \sin \theta_1 \cos \phi)} \quad (62)$$

Substituting for  $P_r$  in equation (46) gives

$$2P_i = P_1 + \dot{W}_P \left[ Z_P + \frac{\rho_1 c_1}{\cos \theta_1 (1 + M_1 \sin \theta_1 \cos \phi)} \right] \quad (63)$$

where  $\dot{W}_P = j \omega W_P$ , and  $P_2 = P_{2i} + P_{2r} =$  fluid pressure on the transmitting side of the panel.

Now  $Z_1$  is the impedance on the terminating side of the panel, so that

$$P_1 = Z_1 \dot{\xi}_1 = Z_1 \dot{W}_P \quad (64)$$

or

$$\dot{W}_P = P_1 / Z_1 \quad (65)$$

Substituting equation (65) into (63), the pressure drop across the panel ( $P_i/P_1$ ) becomes

$$\frac{P_i}{P_1} = \frac{1}{2} \left[ 1 + \frac{P_1 C_1}{Z_1 \cos \theta_1 (1 + M_1 \sin \theta_1 \cos \phi)} + \frac{Z_P}{Z_1} \right] \quad (66)$$

### Transmission Loss of the Treated Panel

The transmission loss of the treated panel is given by

$$TL = 10 \log_{10} \left( \frac{P_4 C_4}{P_1 C_1} \right) \left| \frac{P_i}{P_4} \right|^2 \quad (67)$$

$$= 10 \log_{10} \left( \frac{P_4 C_4}{P_1 C_1} \right) + 10 \log_{10} \left| \frac{P_i}{P_1} \cdot \frac{P_1}{P_2} \cdot \frac{P_2}{P_3} \cdot \frac{P_3}{P_4} \right|^2$$

$$= 10 \log_{10} \left( \frac{P_4 C_4}{P_1 C_1} \right) + 10 \log_{10} \left| \frac{P_i}{P_1} \right|^2 + 10 \log_{10} \left| \frac{P_1}{P_2} \right|^2$$

$$+ 10 \log_{10} \left| \frac{P_2}{P_3} \right|^2 + 10 \log_{10} \left| \frac{P_3}{P_4} \right|^2 \quad (68)$$

Equation (68) says that the total TL is the sum of the TL contributed by each layer and that due to the fluid impedance mismatch. All that remains to be done is to compute the pressure ratios from layer to layer.



The pressure drop across the airgap is

$$\frac{P_1}{P_2} = \frac{(P_{2i} + P_{2r})_{z=0}}{(P_{2i} + P_{2r})_{z=d_2}} = \frac{P_{2i} + P_{2r}}{P_{2i} e^{jk_{23}d_2} + P_{2r} e^{-jk_{23}d_2}} \quad (69)$$

Using equation (41),

$$\frac{P_1}{P_2} = \frac{e^{jk_{23}d_2} + R_2 e^{-jk_{23}d_2}}{1 + R_2} \quad (70)$$

Substituting for  $R_2$  from equation (43) yields, after some straightforward manipulation,

$$\frac{P_1}{P_2} = \frac{\cosh(jk_{23}d_2 + \Psi_2)}{\cosh \Psi_2} \quad (71)$$

where

$$\Psi_2 = \coth^{-1}(Z_B k_{23} / \rho_2 \omega) \quad (72)$$

and  $Z_B$  is the terminating impedance of the airgap, given by equation (44).

The pressure drop across the fiberglass blanket is given by

$$\frac{P_2}{P_3} = \frac{(P_{3i} + P_{3r})_{z=d_3}}{(P_{3i} + P_{3r})_{z=0}} = \frac{P_{3i} e^{-b_3 d_3} + P_{3r} e^{b_3 d_3}}{P_{3i} + P_{3r}} \quad (73)$$

Using equation (32), one gets (after a bit of manipulation)

$$\frac{P_2}{P_3} = \frac{\cosh(b_3 d_3 + \psi_3)}{\cosh \psi_3} \quad (74)$$

where

$$\psi_3 = \coth^{-1}(Z_3/Z_A) \quad (75)$$

$Z_3$  is the terminating impedance of the blanket and is given by equation (29).

Finally, the pressure drop across the septum is

$$\frac{P_3}{P_4} = \frac{(P_{3i} + P_{3r})_{\bar{z}=0}}{(P_4)_{z=d}} = \frac{P_{3i} + P_{3r}}{P_4} \quad (76)$$

Using equations (22) and (26) and (27)

$$\frac{P_3}{P_4} = \frac{j\omega(Z_t + Z_4)W_t}{j\omega Z_4 W_t} = 1 + \frac{Z_t}{Z_4} \quad (77)$$

where  $Z_4$  is the impedance looking into the interior and is given by equation (29).

#### Extension to an Arbitrary Arrangement of Layers

The above results can be reinterpreted so that they can be applied to an arbitrary arrangement of blankets, airgaps, panels, and septa. The generalization goes as follows:

(i) Airgap

The TL across the air gap is given by

$$\Delta TL = 10 \log_{10} \left| \frac{\cosh(j k_{23} d_A + \psi_2)}{\cosh \psi_2} \right|^2 \quad (78)$$

where

$$\psi_2 = \coth^{-1} (Z_T / Z_I) \quad (79)$$

$$Z_T = \text{terminating impedance of air gap} \quad (80)$$

$$Z_I = \text{input impedance to airgap}$$

$$= \left( \frac{\rho_2 \omega}{k_{23}} \right) \coth(j k_{23} d_A + \psi_2) \quad (81)$$

$$d_A = \text{depth of airgap}$$

(ii) Fiberglass Blanket

The TL contribution from the blanket is

$$\Delta TL = 10 \log_{10} \left| \frac{\cosh(b_3 d_B + \psi_3)}{\cosh \psi_3} \right| \quad (82)$$

where

$$\psi_3 = \coth^{-1} (Z_3 / Z_A) \quad (83)$$

$Z_3$  = terminating impedance of blanket

$Z_A$  = characteristic impedance of blanket

$$= -j (K d_3 / \omega Y) \quad (84)$$

$d_3$  = thickness of blanket

(iii) Septum

The TL increment provided by a septum is given by

$$\Delta TL = 10 \log_{10} \left| 1 + \frac{Z_t}{Z_4} \right|^2 \quad (85)$$

where

$$Z_t = j \omega m_t = \text{impedance of septum} \quad (86)$$

$Z_4$  = terminating impedance of septum

(iv) Orthotropic Trim Panel

For a trim panel, equation (85) is still valid, but now

$Z_t$  = impedance of trim panel

$$= j \omega m_t \left[ 1 - (D_x k_{px}^4 + 2 D_{xy} k_{px}^2 k_{py}^2 + D_y k_{py}^4) / (m_t \omega^2) \right] \quad (87)$$

$Z_4$  = terminating impedance of trim panel

(v) Bare Orthotropic Panel

The TL increment of the bare untreated panel is given by

$$\Delta TL = 10 \log_{10} \left[ \frac{1}{2} + \frac{\rho_1 c_1}{2 Z_1 \cos \theta_1 (1 + M_1 \sin \theta_1 \cos \phi)} + \frac{Z_p}{Z_1} \right] \quad (88)$$

where

$Z_1$  = terminating impedance of panel

$Z_p$  = impedance of panel

$$= j\omega m_p \left[ 1 - (1 + j\eta) (D_x k_{px}^4 + 2 D_{xy} k_{px}^2 k_{py}^2 + D_y k_{py}^4) / (m_p \omega^2) \right]$$

(89)

where  $\eta$  = loss factor of panel

$\rho_1 c_1$  = characteristic impedance of external air

$M_1$  = external flow Mach number

$m_p$  = mass/area of panel

(vi) Extension to a Laminated Composite Panel

Equation (88) can be extended to include a laminated composite panel if the panel impedance,  $Z_p$ , of equation (89) is suitably modified. The differential equation for a composite panel is

$$\begin{aligned} D_{11} \frac{\partial^4 w}{\partial x^4} + 4 D_{16} \frac{\partial^4 w}{\partial x^3 \partial y} + 2(D_{12} + 2D_{66}) \frac{\partial^4 w}{\partial x^2 \partial y^2} + 4 D_{26} \frac{\partial^4 w}{\partial x \partial y^3} \\ + D_{22} \frac{\partial^4 w}{\partial y^4} + m_p \frac{\partial^2 w}{\partial t^2} = p(x, y, t) \end{aligned} \quad (90)$$

where  $D_{ij}$  are the anisotropic plate rigidity values that relate the internal bending and twisting moments of the plate to the twists and curvatures they induce. The expressions for  $D_{ij}$  are well known and given in standard texts (e.g., ref. 4, p. 155).

Corresponding to equation (90), the impedance for a laminated composite panel is given by

$$\begin{aligned} Z_p = j\omega m_p \left\{ 1 - (1+j\eta) \left[ D_{11} k_{px}^4 + 4 D_{16} k_{px}^3 k_{py} + \right. \right. \\ \left. \left. 2(D_{12} + 2D_{66}) k_{px}^2 k_{py}^2 + 4 D_{26} k_{px} k_{py}^3 + D_{22} k_{py}^4 \right] \right\} \end{aligned} \quad (91)$$

### Field-Incidence Transmission Loss

From the pressure drop across the panel and across each individual treatment layer, the transmission coefficient  $\tau(\theta, \phi, \omega)$  can be defined as

$$\tau(\theta, \phi, \omega) = \left( \frac{P_E C_E}{P_I C_I} \right) \left| \frac{P_i}{P_1} \cdot \frac{P_1}{P_2} \cdot \frac{P_2}{P_3} \cdot \dots \right| \quad (92)$$

where the subscript E refers to conditions on the incident (exterior) side and I to the conditions on the transmitting (interior) side. The field-incidence transmission coefficient  $\bar{\tau}(\omega)$  is then computed from (ref. 5, p. 262)

$$\bar{\tau}(\omega) = \frac{\int_{\phi=0}^{2\pi} \int_{\theta=0}^{\theta_L} \tau(\theta, \phi, \omega) \cos \theta, \sin \theta, d\theta, d\phi}{\int_{\phi=0}^{2\pi} \int_{\theta=0}^{\theta_L} \cos \theta, \sin \theta, d\theta, d\phi} \quad (93)$$

The integral in the numerator of equation (93) has been evaluated numerically, that in the denominator was integrable in closed form. Thus, equation (93) can be put into the form

$$\bar{\tau}(\omega) = \frac{1}{2\pi \sin^2 \theta_L} \int_0^{2\pi} \int_0^{\theta_L} \tau(\theta, \phi, \omega) \sin 2\theta, d\theta, d\phi \quad (94)$$

In the numerical integration, Simpson's 1/3-Rule was used with 15° - angular\* increments in  $\theta_1$  and  $\phi$ .  $\theta_L$  is the "limiting angle of incidence" and is taken as 78° for field-incidence calculations.

---

\*Early runs were made with 5° intervals, but 15° intervals were found to give comparable accuracy and used less computer time.

Finally, in order to compare with experimental results, there must be a conversion to 1/3-octave frequency bands. The transmission coefficient in equation (94) is calculated for a single frequency. The conversion to 1/3-octave values was accomplished in the same manner as done by Mixson, Roussos, et al<sup>6,7</sup>, wherein the 1/3-octave band transmission loss was computed from

$$TL = 10 \log_{10} \left[ \frac{\sum_{f=f_L}^{f_U} S(f) \Delta f}{\sum_{f=f_L}^{f_U} \bar{T}(f) S(f) \Delta f} \right] \quad (95)$$

where  $f = \omega/2\pi =$  frequency,  $f_L$  and  $f_U$  are the lower and upper bounds of the 1/3-octave frequency bands,  $S(f)$  is the narrow band experimentally-determined power spectral density of the incident pressure, and  $\Delta f$  is the width of the narrow band. The transmission coefficient was evaluated at the center frequency of each narrow band of data.

#### CONCLUDING REMARKS

The preceding model has been applied to a number of cases, and the numerical results compared with available test data. In all of these cases, the external flow was zero.

Figures 2, 3, and 4 are comparisons with test data generated by F. Balena of Lockheed-California Company and reported in reference 8 as figures 42, 44, and 45, respectively. These cases consist of panels treated with fiberglass blankets with, and without, trim panels. The trim panels are modeled as



septa, and there is an airgap between the skin panel and the fiberglass blanket. Appropriate dimensions and properties are given on figures 2, 3, and 4. Agreement between the calculations and the Lockheed data is seen to be fairly good.

The model was also compared with experimental data reported by Mixson, Roussos, et al<sup>6</sup>, in figures 5 through 11. The experimental data in question is presented in reference 6 as figures 15 and 17 (Figures 12 and 13 of reference 7). In general, the theory does predict the trends observed experimentally. In some cases there is good agreement, e.g. figures 5 and 6; in other cases, there is lesser agreement, e.g. figures 9, 10, and 11. This may be due to uncertainties in some of the properties used for the plywood trim panel and for the fiberglass blanket.

A list of the physical properties assumed in these calculations is given in Table I. Fiberglass blankets were assumed to be in two layers, each layer consisting of a 2.54 cm (1 in.) layer of fiberglass terminated with a vinyl septum. When a fiberglass blanket was employed, it was assumed that there was a 4.06 cm (1.60 in.) airgap between the skin panel and the blanket. When present, the plywood trim panel was assumed to be in contact with the terminating side of the fiberglass. Numbers run with an airgap between the blanket and plywood trim panel did not at all agree with test data and predicted TL's higher than those obtained experimentally. It was only when the trim panel was in contact with the fiberglass blanket did the model predict TL's consistent with experimental values. For this reason, the airgap between the blanket and the test panel was taken to be the distance between the test panel and the trim panel, 9.14 cm (3.60 in.), minus the thickness of the blanket, 5.08 cm (2.0 in.).

Figures 12, 13, and 14 show a comparison between calculated TL and experimental values for three typical laminated composite panels, viz., Kevlar/epoxy, graphite/epoxy, and fiberglass/epoxy. These figures have been presented as figures 5, 6, and 7 in reference 9, but are repeated here to make this document self-contained. Each figure shows comparisons for 8-ply and 16-ply panels, and also a comparison with TL computed using equations appropriate for field-incidence mass-law behavior. Agreement between the infinite panel theory presented in this report and the test results is seen to be quite good for all three materials, and even includes the dip in TL which occurs when coincidence effects become important and mass-law predictions breakdown. The fiber orientations for the 8-ply panels were balanced symmetric layups of  $[0^\circ, 90^\circ, 0^\circ, 90^\circ]$ , and for the 16-ply panels balanced symmetric layups of  $[45^\circ, -45^\circ, 45^\circ, -45^\circ, 45^\circ, -45^\circ, 45^\circ, -45^\circ]$ .

APPENDIX A

Derivation of Equation (3)

Beranek, in equation (9) of reference 2 has shown that the sound pressure in the tile/blanket can be written as

$$\left\{ \left( D^2 - \frac{j\omega}{Q} Z_2 \right) \left( D^2 - \frac{j\omega Y}{K} Z_1 \right) - D^2 \left[ \frac{j\omega \tau_{12} (1-Y)}{Q} \right] + \frac{\omega^2 \tau_{12}^2 Y^2}{KQ} \right\} p = 0 \quad (A-1)$$

where  $D = \partial/\partial x$  and  $j\omega = \partial/\partial t$  (for harmonic motion). The quantities  $K, Q, Y, \tau_{12}$  have the same meaning as in Beranek's paper.

Equation (A-1) can be rearranged into the form

$$\left\{ KQ D^4 - j\omega D^2 \left[ Z_2 K + Z_1 Y Q + (1-Y) \tau_{12} K \right] - Y \omega^2 (Z_1 Z_2 - \tau_{12}^2 Y) \right\} p = 0 \quad (A-2)$$

The characteristic equation has roots

$$\lambda^2 = j\omega \left[ \frac{Z_2 K + Z_1 Y Q + (1-Y) \tau_{12} K}{KQ} \right] \left\{ \frac{1}{2} \pm \frac{1}{2} \sqrt{1 - \frac{4KQY(Z_1 Z_2 - \tau_{12}^2 Y)}{Z_2 K + Z_1 Y Q + (1-Y) \tau_{12} K}} \right\} \quad (A-3)$$

For  $4KQY(Z_1 Z_2 - \tau_{12}^2 Y) \ll [Z_2 K + Z_1 Y Q + (1-Y) \tau_{12} K]$ , Beranek gave a binomial expansion of the radical. Two roots were obtained, viz.,  $\lambda = \pm a$  and  $\lambda = \pm b$ ,

where

$$a = (j\omega/Q)^{1/2} \left[ Z_2 + (1-Y) \tau_{12} \right]^{1/2} \quad (A-4)$$

$$b \doteq (j\omega/k)^{1/2} \left[ \frac{Y(Z_1 Z_2 - \tau_{12}^2 Y)}{Z_2 + (1-Y)\tau_{12}} \right]^{1/2} \quad (\text{A-5})$$

In equations (A-4) and (A-5),  $K > 20Q$  (for most common materials,  $K > 100Q$ ). When  $(\omega\rho_m)^2$  is large compared to the square of the real part of  $Z_2$ , Beranek has shown that

$$b \doteq (j\omega/k)^{1/2} \left[ (R_1 + j\omega\rho_0 k) Y \right]^{1/2} \quad (\text{A-6})$$

Equations (A-4), (A-5) and (A-6) are Beranek's equations (13), (14), and (15) of reference 2.

Equation (A-2) can be factored into the form

$$(D^2 - a^2)(D^2 - b^2)p = 0 \quad (\text{A-7})$$

the general solution to which is given by\*

$$p = Ae^{ax} + Be^{-ax} + Ce^{bx} + De^{-bx} \quad (\text{A-8})$$

where  $a$  and  $b$  can be seen to be propagation constants. Beranek (ref. 2) states that when  $K > 20Q$  (for a soft blanket) "... one of the two waves, expressed by the propagation constant  $a$ , ... is highly attenuated, travels with low velocity, and usually may be neglected." Thus, in its principal physical effect, equation (A-7) can be replaced by

$$(D^2 - b^2)p = 0 \quad (\text{A-9})$$

---

\*Multiplication of  $p$  by  $e^{j\omega t}$  is understood

or,

$$\left[ D^2 - \frac{j\omega Y}{K} (R_1 + j\omega \rho_0 k) \right] p = 0 \quad (\text{A-10})$$

Replacing  $D$  by  $\partial/\partial x$ , and  $j\omega t$  by  $\partial/\partial t$ , the sound pressure equation is given by

$$\frac{\partial^2 p}{\partial x^2} = \frac{R_1 Y}{K} \frac{\partial p}{\partial t} + \frac{\rho_0 k Y}{K} \frac{\partial^2 p}{\partial t^2} \quad (\text{A-11})$$

This is the one-dimensional equation for sound-wave propagation in an acoustical blanket. For three-dimensional propagation, equation (A-11) can be expanded to the form

$$\frac{\partial^2 p}{\partial x^2} + \frac{\partial^2 p}{\partial y^2} + \frac{\partial^2 p}{\partial z^2} = \left( \frac{\rho_0 k Y}{K} \right) \frac{\partial^2 p}{\partial t^2} + \left( \frac{R_1 Y}{K} \right) \frac{\partial p}{\partial t} \quad (\text{A-12})$$

Equation (A-12) is equation (3) in the main body of this report.

## APPENDIX B

### Derivation of Equation (24)

According to Beranek (ref. 2), if  $u$  is the particle velocity for the acoustical blanket (treated as a continuum),  $u_1$  the particle velocity of the air and  $u_2$  the velocity of the fiber material, then (ref. 2 after eq. (20))

$$u = - \{ Y u_1 + (1-Y) u_2 \} \quad (\text{B-1})$$

where  $Y$  is the porosity of the blanket. For a soft acoustic blanket,  $Y \doteq 1$ , so that

$$u \doteq -Y u_1 \quad (\text{B-2})$$

From continuity considerations (Beranek's equation (3)),

$$\frac{\partial u_1}{\partial z} + \frac{1}{K} \frac{\partial p}{\partial t} - \left( \frac{1-Y}{QY} \right) \frac{\partial p_2}{\partial t} = 0 \quad (\text{B-3})$$

where  $p$  is the sound pressure in the air and  $p_2$  the "average excess pressure exerted by a sound wave against the matter contained in the material." For  $Y \doteq 1$ , equation (B-3) reduces to

$$\frac{\partial u_1}{\partial z} = - \frac{1}{K} \frac{\partial p}{\partial t} \quad (\text{B-4})$$

Combining equations (B-2) and (B-4),

$$\frac{\partial u}{\partial z} = \frac{Y}{K} \frac{\partial p}{\partial t} \quad (\text{B-5})$$

Finally, substituting

$$u = U_{3i} \exp[j(\omega t - k_{3x}x - k_{3y}y)] e^{b_3(z-d)} \quad (\text{B-6})$$

$$p = P_{3i} \exp[j(\omega t - k_{3x}x - k_{3y}y)] e^{b_3(z-d)}$$

into (B-5) gives

$$b_3 U_{3i} = \frac{Y}{K} j\omega P_{3i}$$

or

$$U_{3i} = \frac{j\omega Y}{K b_3} = P_{3i} / Z_A \quad (\text{B-7})$$

where

$$Z_A = \frac{K b_3}{j\omega Y} = -j \left( \frac{K b_3}{\omega Y} \right) \quad (\text{B-8})$$

Equations (B-7) and B-8) appear in the main text as equations (24) and (25), respectively.

APPENDIX C

Calculation of  $R_2$ , Equation (43)

As per equation (42),

$$R_2 = \frac{(1-z_R)P_{3i} e^{-bd} + (1+z_R)P_{3r} e^{bd}}{(1+z_R)P_{3i} e^{-bd} + (1-z_R)P_{3r} e^{bd}} \quad (C-1)$$

where  $bd = b_3 d_3$ .

$$\frac{P_{3i}}{P_{3r}} = \frac{z_3 + z_A}{z_3 - z_A} = \frac{\hat{z} + 1}{1 - \hat{z}} \quad (C-2)$$

where

$$\hat{z} = z_A / z_3$$

Substituting equation (C-2) into (C-1) results in

$$R_2 = \frac{1 + \hat{z} \tanh bd - z_R \tanh bd - \hat{z} z_R}{1 + \hat{z} \tanh bd + z_R \tanh bd + \hat{z} z_R} \quad (C-3)$$

or

$$R_2 = \frac{1 - z_R \tanh (bd + \psi_B)}{1 + z_R \tanh (bd + \psi_B)} \quad (C-4)$$

where

$$\psi_B = \coth^{-1} (z_3 / z_A) \quad (C-5)$$



Substituting for  $Z_R$  as per equation (39) gives

$$R_2 = \left(1 - \frac{\rho_2 \omega}{k_{23} Z_B}\right) / \left(1 + \frac{\rho_2 \omega}{k_{23} Z_B}\right) \quad (C-6)$$

## REFERENCES

1. Mixson, J. S.; Barton, C. K.; Piersol, A. G.; and Wilby, J. F.: Characteristics of Propeller Noise on an Aircraft Fuselage Related to Interior Noise Transmission. AIAA Paper No. 79-0646, 5th AIAA Aeroacoustics Conference, Seattle, Washington, March 1979.
2. Beranek, L. L.: Acoustical Properties of Homogeneous, Isotropic Rigid Tiles and Flexible Blankets. *Journal of the Acoustical Society*, vol. 19, no. 4, July 1947.
3. Beranek, L. L.; and Work, G. A.: Sound Transmission Through Multiple Structures Containing Flexible Blankets. *Journal of Acoustical Society of America*, vol. 21, no. 4, July 1949, pp. 419-428.
4. Jones, R. M.: *Mechanics of Composite Materials*. New York: McGraw-Hill, 1975.
5. Beranek, L. L. (Ed.): *Noise and Vibration Control*. New York: McGraw-Hill, 1971.
6. Mixson, J. S.; Roussos, L. A.; Barton, C. K.; Vaicaitas, R.; and Slazak, M.: Laboratory Study of Efficient Add-On Treatments for Interior Noise Control in Light Aircraft. Presented at AIAA 7th Aeroacoustics Conference, Paper No. 81-1969, October 1981.
7. Mixson, J. S., Roussos, L. A., Barton, C. K., Vaicaitis, R., and Slazak, M.: Laboratory Study of Add-on Treatments for Interior Noise Control in Light Aircraft. *Journal of Aircraft*, vol. 20, no. 6, June 1983, pp. 516-522.
8. Revell, J. D.; Balena, F. J.; and Koval, L. R.: Analytical Study of Interior Noise Control by Fuselage Design Techniques on High-Speed Propeller-Driven Aircraft. NASA CR-159222, July 1978. (Figs. 44 and 45 are also given as fig. 6 in "Analysis of Interior Noise-Control

Treatments for High-Speed Propeller Driven Aircraft," J. of Aircraft, vol. 19, no. 1, January 1982, by the same authors.)

9. Roussos, L. A., Grosveld, F. W., Koval, L. R., and Powell, C. A.: Noise Transmission Characteristics of Advanced Composite Structural Materials. Presented at AIAA 8th Aeroacoustics Conference, Paper No. 83-0694 April, 1983.

TABLE I.- PHYSICAL DATA EMPLOYED FOR FIGURES 5-11

Skin Panel:  $D_x = 9754$ ,  $D_{xy} = 5.3$ ,  $D_y = 31940$  N-m

$m_p = 4.06$  Kg/m<sup>2</sup>,  $\eta = 0.05$  (undamped)

$m_p = 5.51$  Kg/m<sup>2</sup>,  $\eta = 0.10$  (damped)

Airgap:  $d_A = 4.06$  cm (1.60 in.),  $\rho_A = 1.25$  Kg/m<sup>3</sup>,  $C_A = 343$  m/s

Blanket\* (each layer):  $\gamma = 0.99$ ,  $\rho_0 = 1.25$  kg/m<sup>3</sup>,  $k = 1.01$ ,  $d_B = 2.54$  cm

$Rl = 4.1 \times 10^4$  mks Rayl/m (104 cgs Rayl/in.),  $\rho_m = 19.6$  Kg/m<sup>3</sup>

Septum:  $m_s = 1.07$  Kg/m<sup>2</sup> (one per layer of fiberglass)

Trim Panel:  $TD_x = 90.8$ ,  $TD_{xy} = 22.58$ ,  $TD_y = 11.67$  N-m

$m_t = 2.10$  Kg/m<sup>2</sup>,  $\eta = 0.10$  (undamped)

$m_t = 3.54$  Kg/m<sup>2</sup>,  $\eta = 0.15$  (damped)

\* The value of  $K$ , the compressibility of the air in the blanket, corresponds to figure 10.6, p. 254 of Beranek (ref. 6).  $K$  ranges from  $10^5$  N/m<sup>2</sup> (isothermal) at low frequencies to  $1.4 \times 10^5$  N/m<sup>2</sup> (adiabatic) at high frequencies.

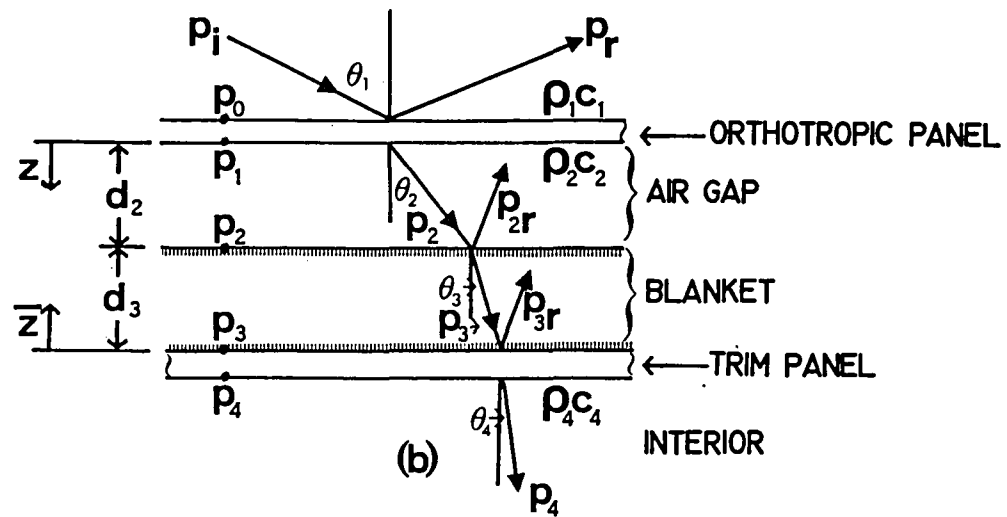
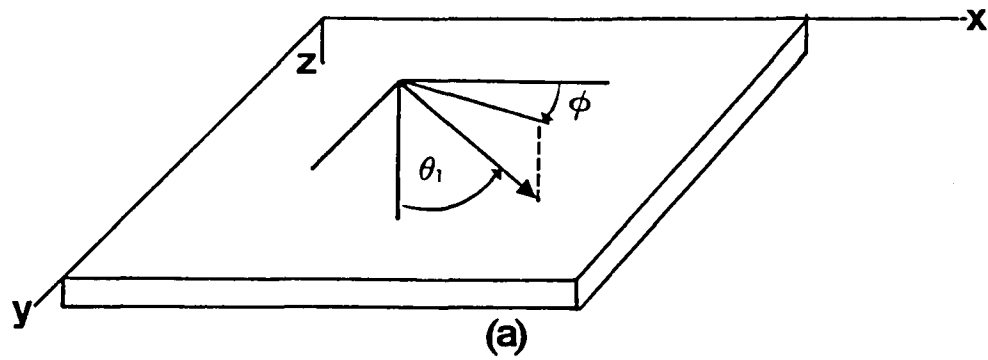


Figure 1.- Geometry of problem.

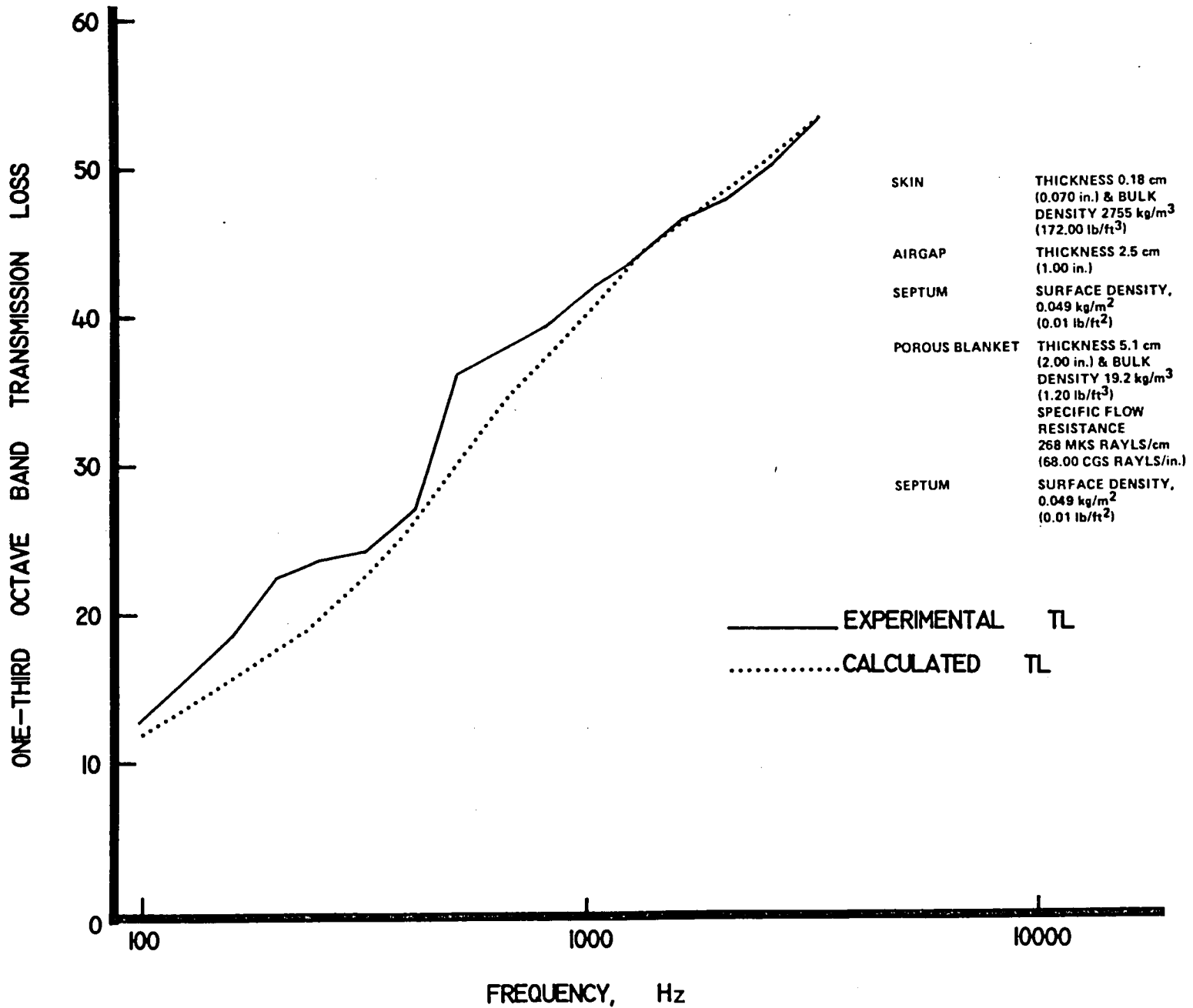


Figure 2.- Panel transmission loss; 7.6 cm (3 in.) wall spacing with a 19.2 Kg/m<sup>3</sup> (1.2 pcf) blanket.

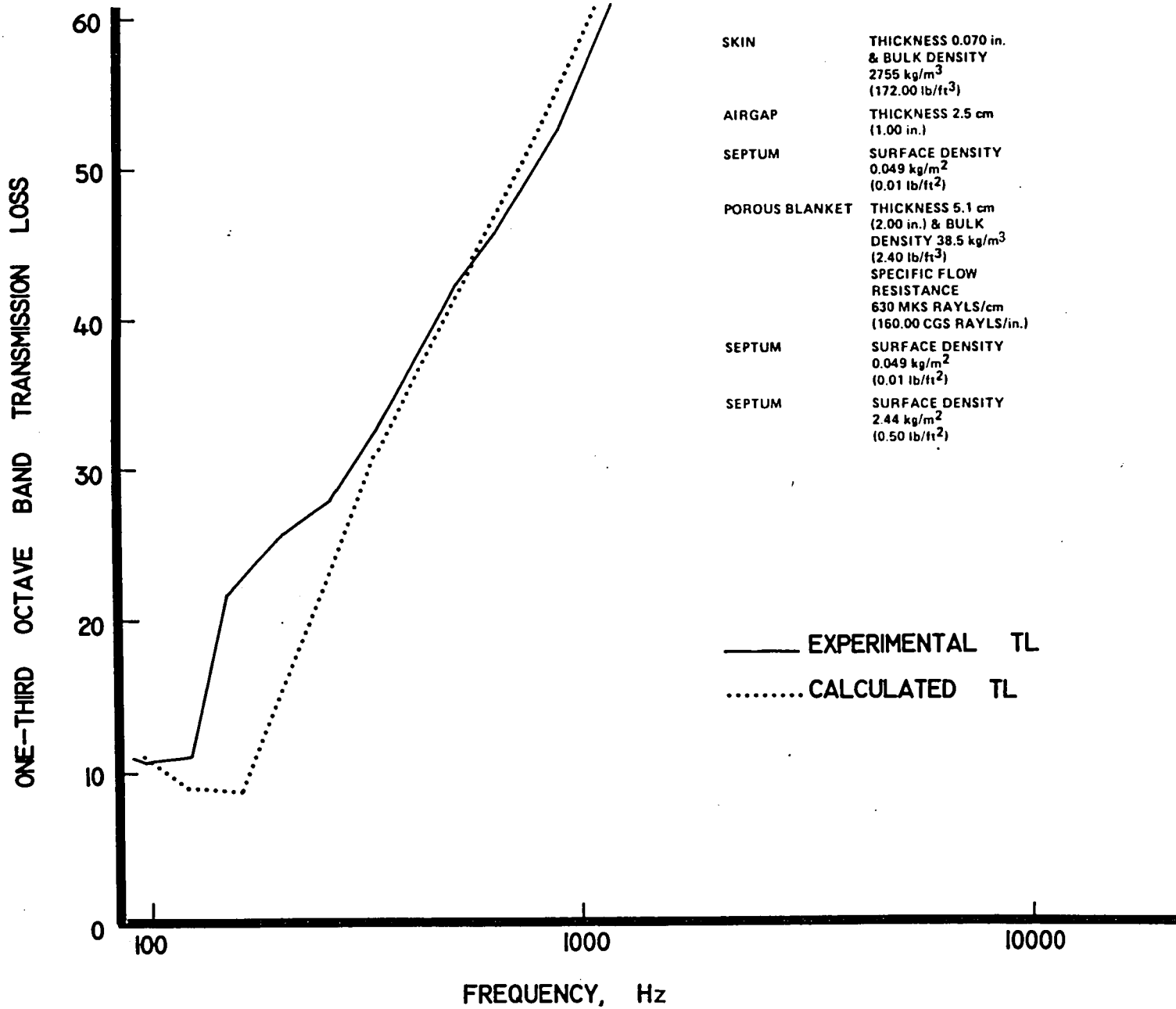


Figure 3.- Panel transmission loss; 7.6 cm (3 in.) wall spacing with a 38.5 Kg/m<sup>3</sup> (2.4 pcf) blanket and a 2.44 Kg/m<sup>2</sup> (0.50 psf) septum.

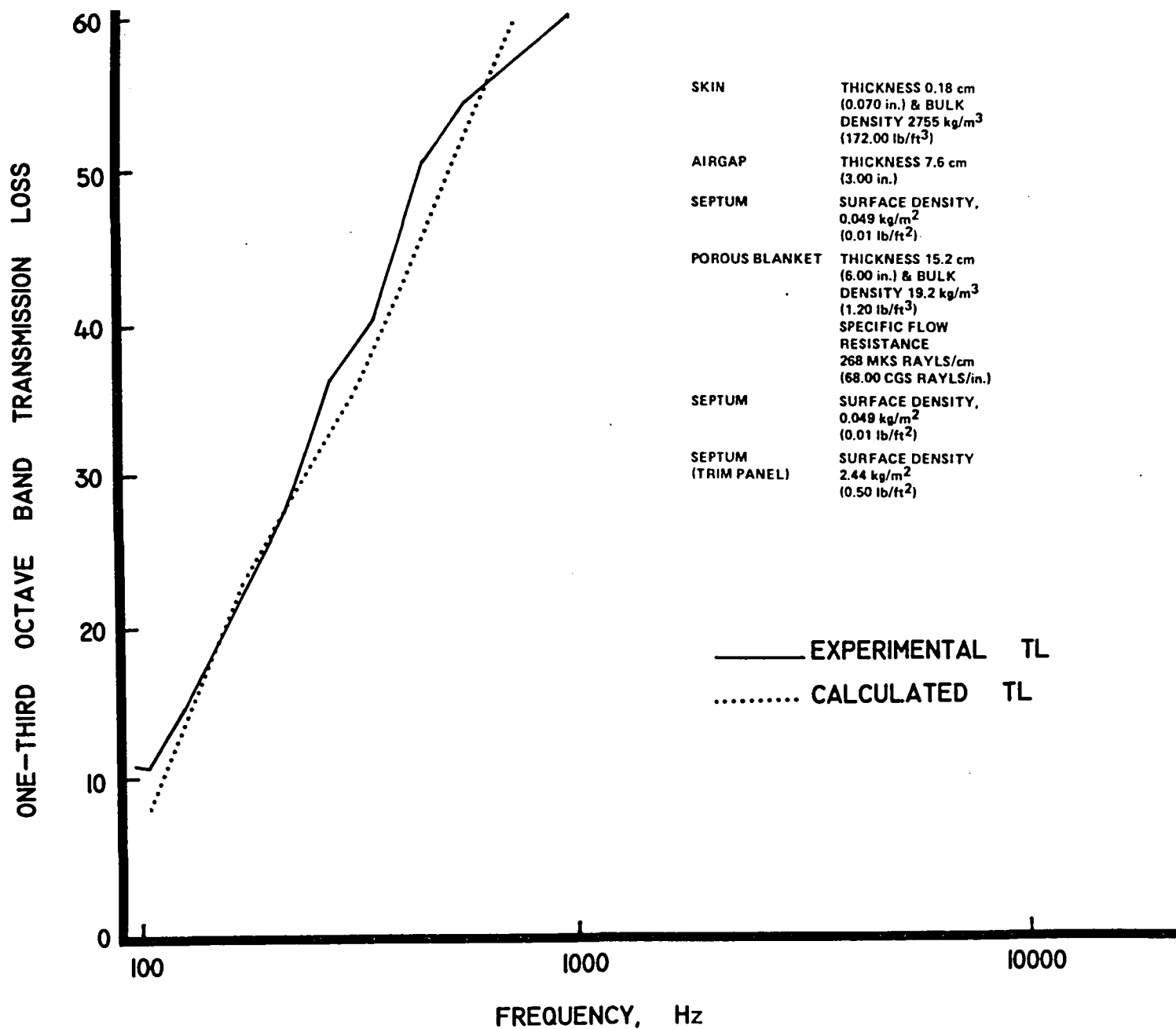


Figure 4.- Panel transmission loss; 22.9 cm (9 in.) wall spacing with a 19.2 Kg/m<sup>3</sup> (1.2 pcf) blanket and 2.44 Kg/m<sup>2</sup> (0.50 psf) septum.



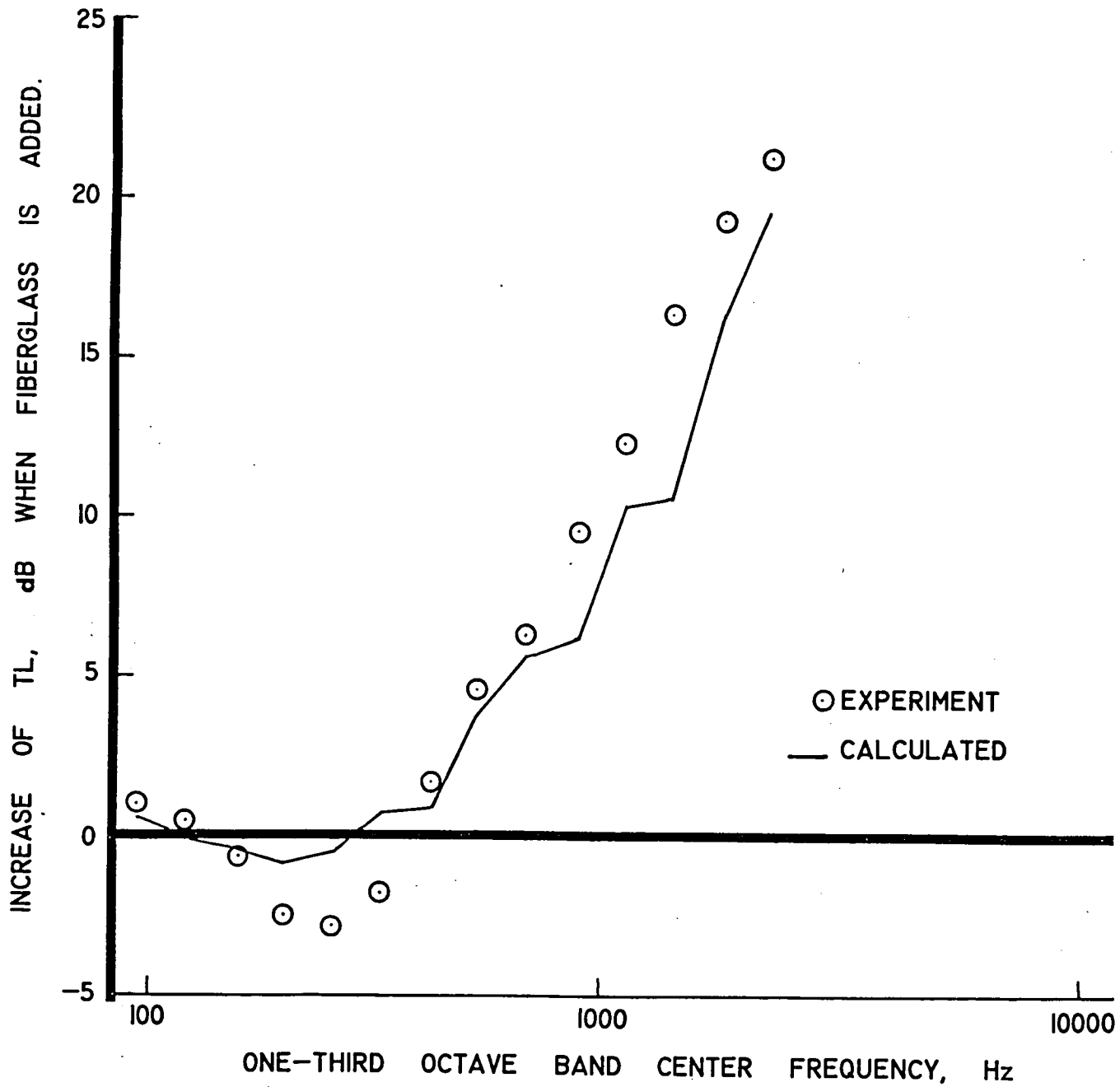


Figure 5.- Insertion loss of fiberglass treatment; no initial treatment.

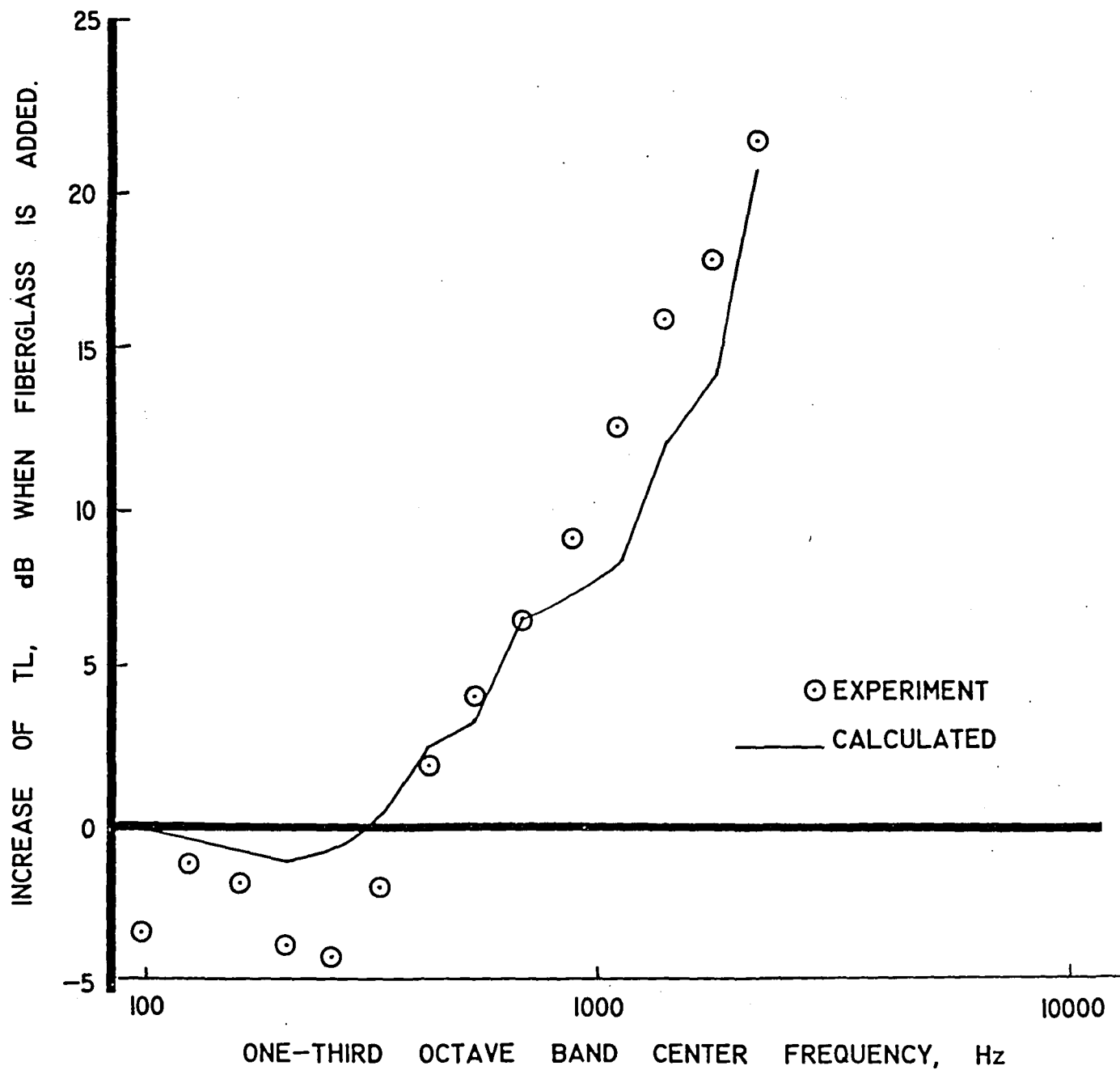


Figure 6.- Insertion loss of fiberglass treatment;  
initial treatment is panel damping.

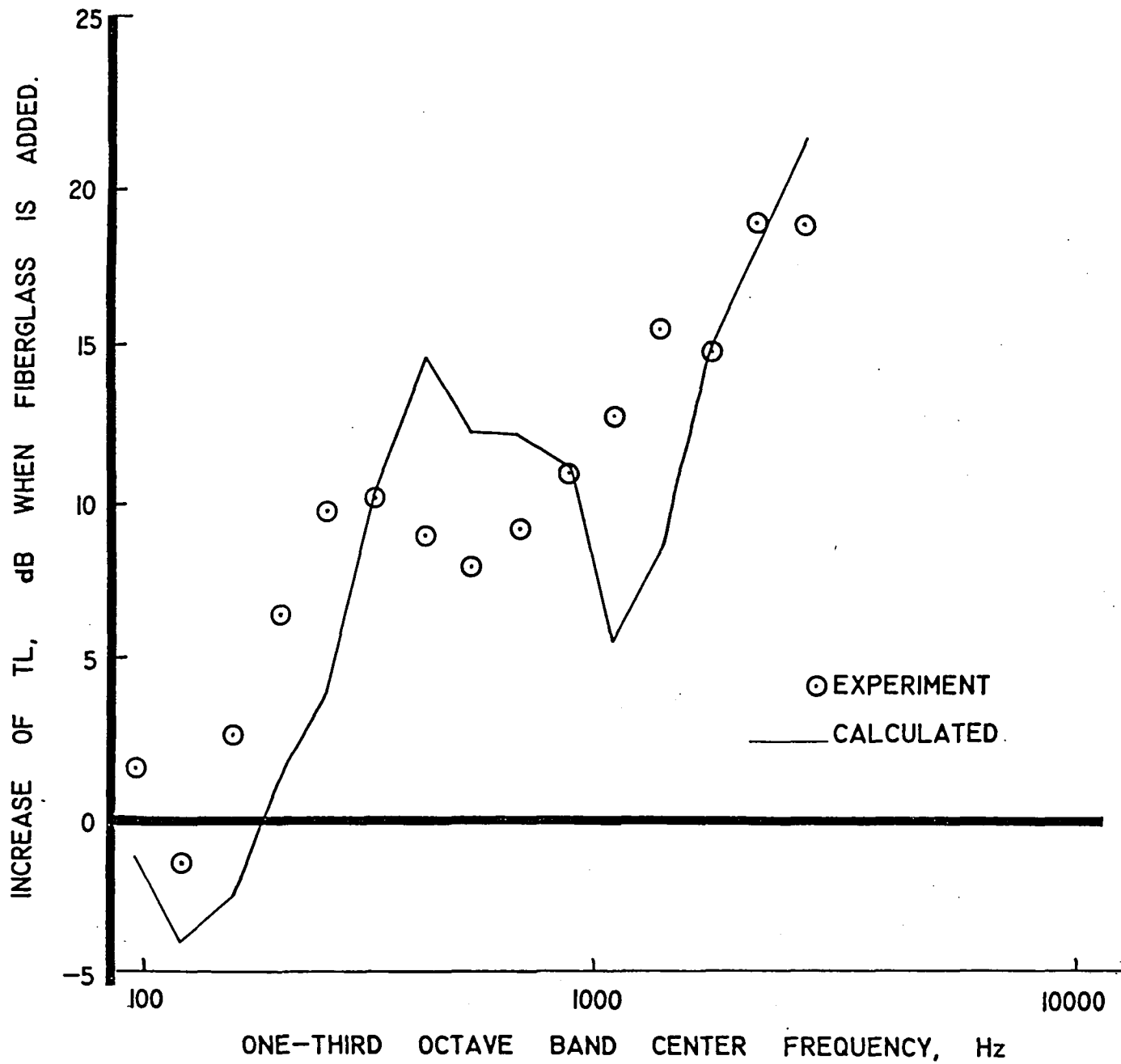


Figure 7.- Insertion loss of fiberglass treatment;  
initial treatment is trim panel.

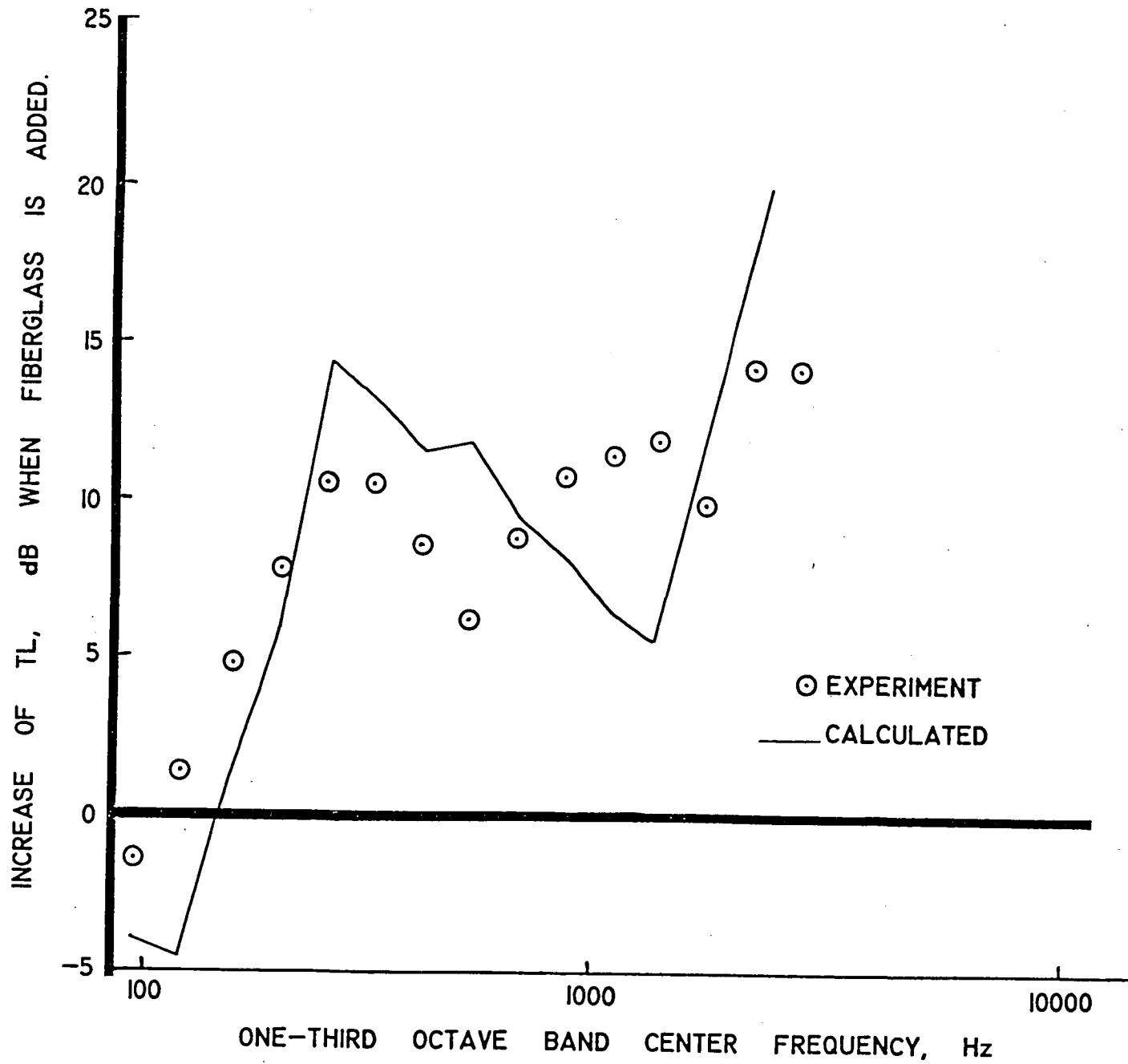


Figure 8.- Insertion loss of fiberglass treatment; initial treatment is panel damping and damped trim panel.

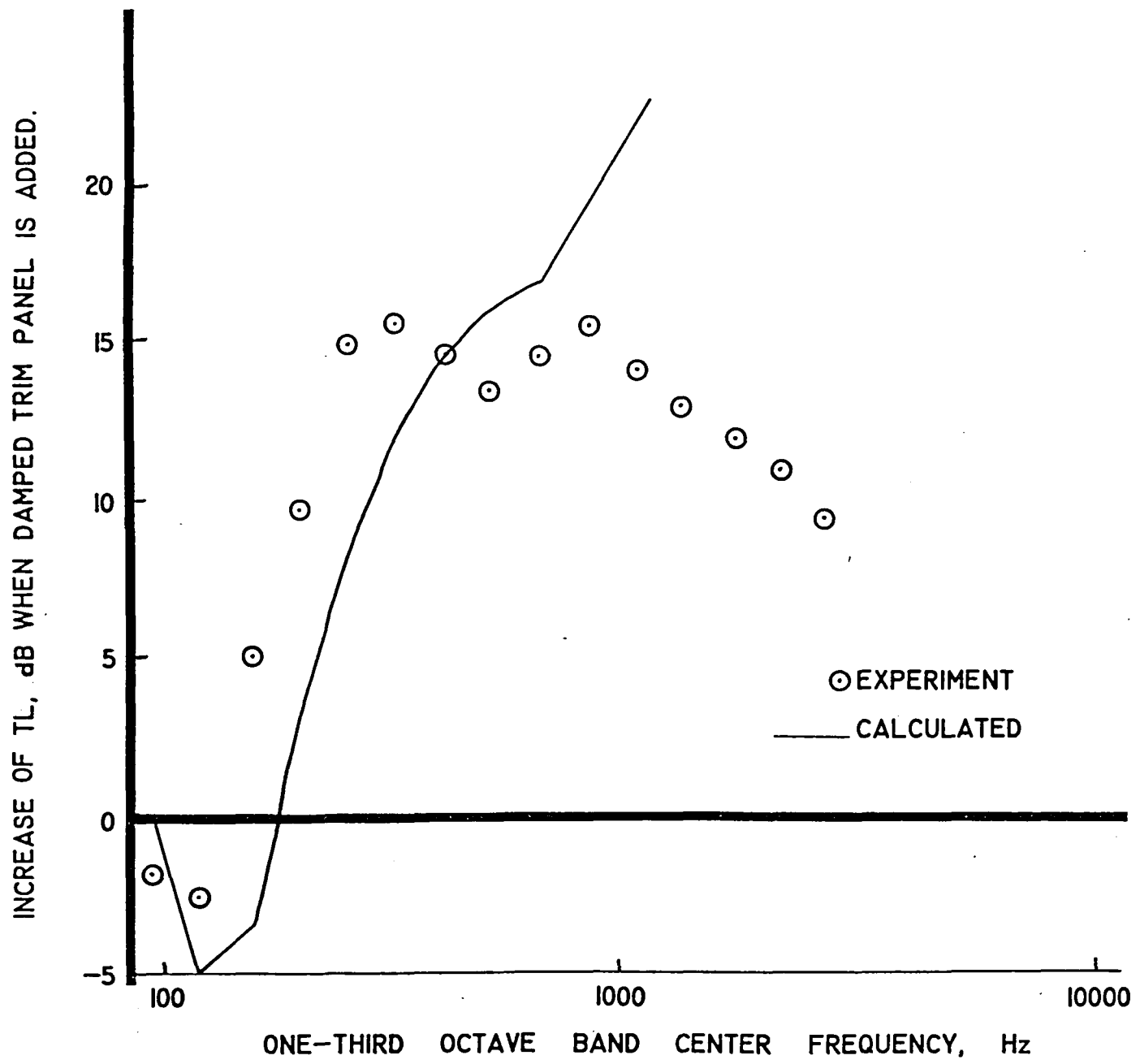


Figure 9.- Insertion loss of damped trim panel treatment; initial treatment is fiberglass.

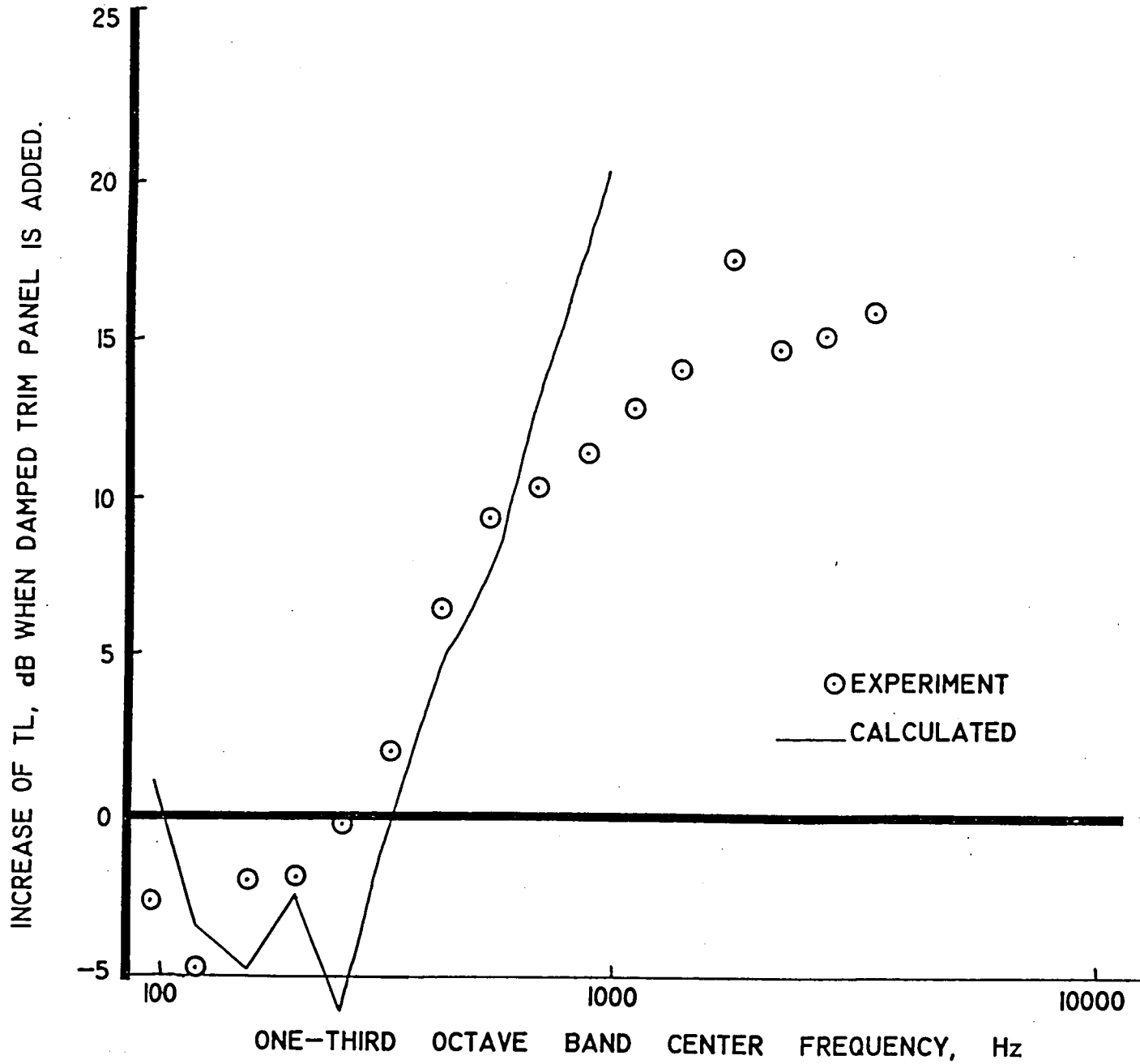


Figure 10.- Insertion loss of damped trim panel treatment; initial treatment is panel damping.

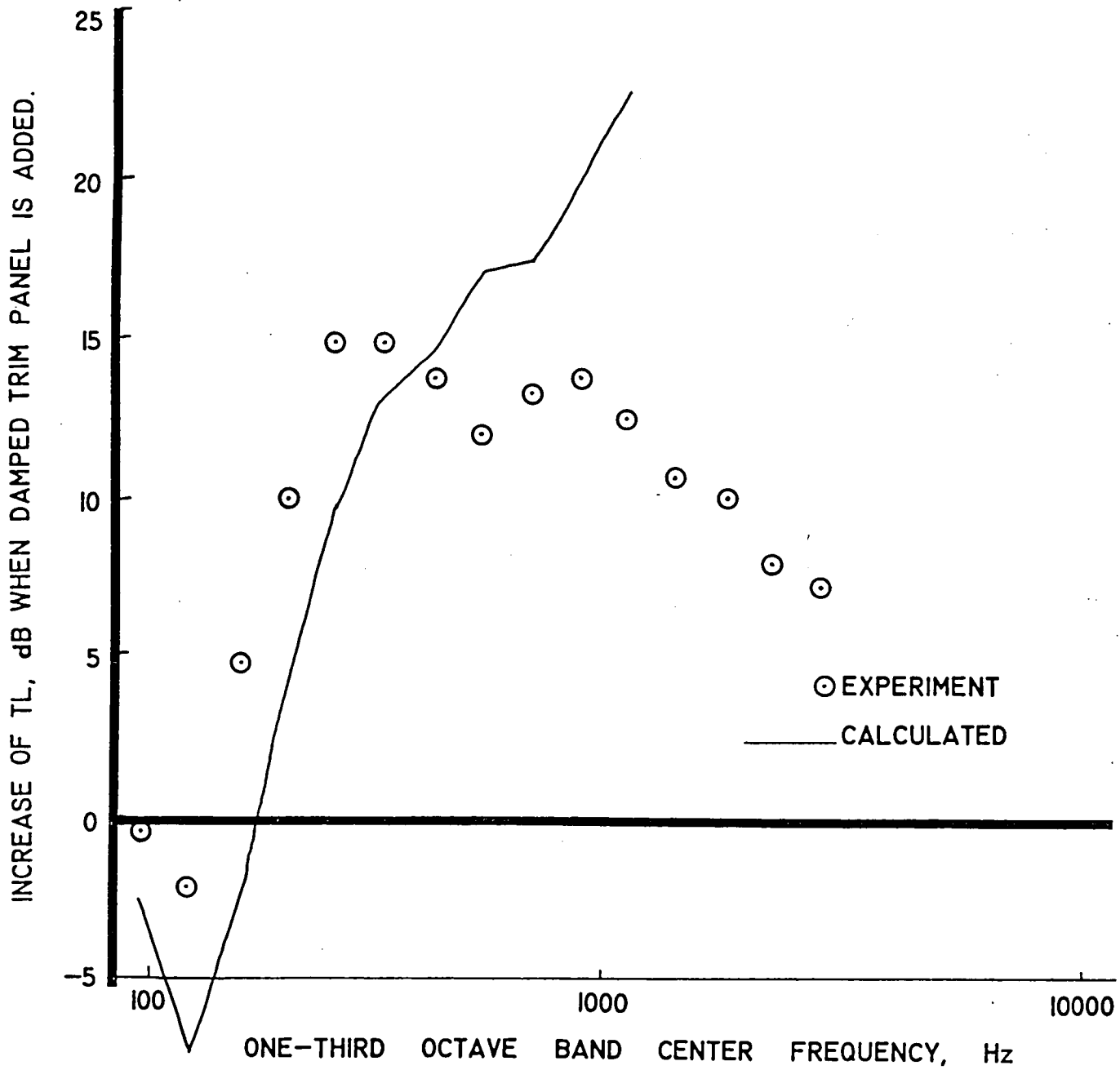


Figure 11.- Insertion loss of damped trim panel treatment; initial treatment is panel damping and fiberglass.

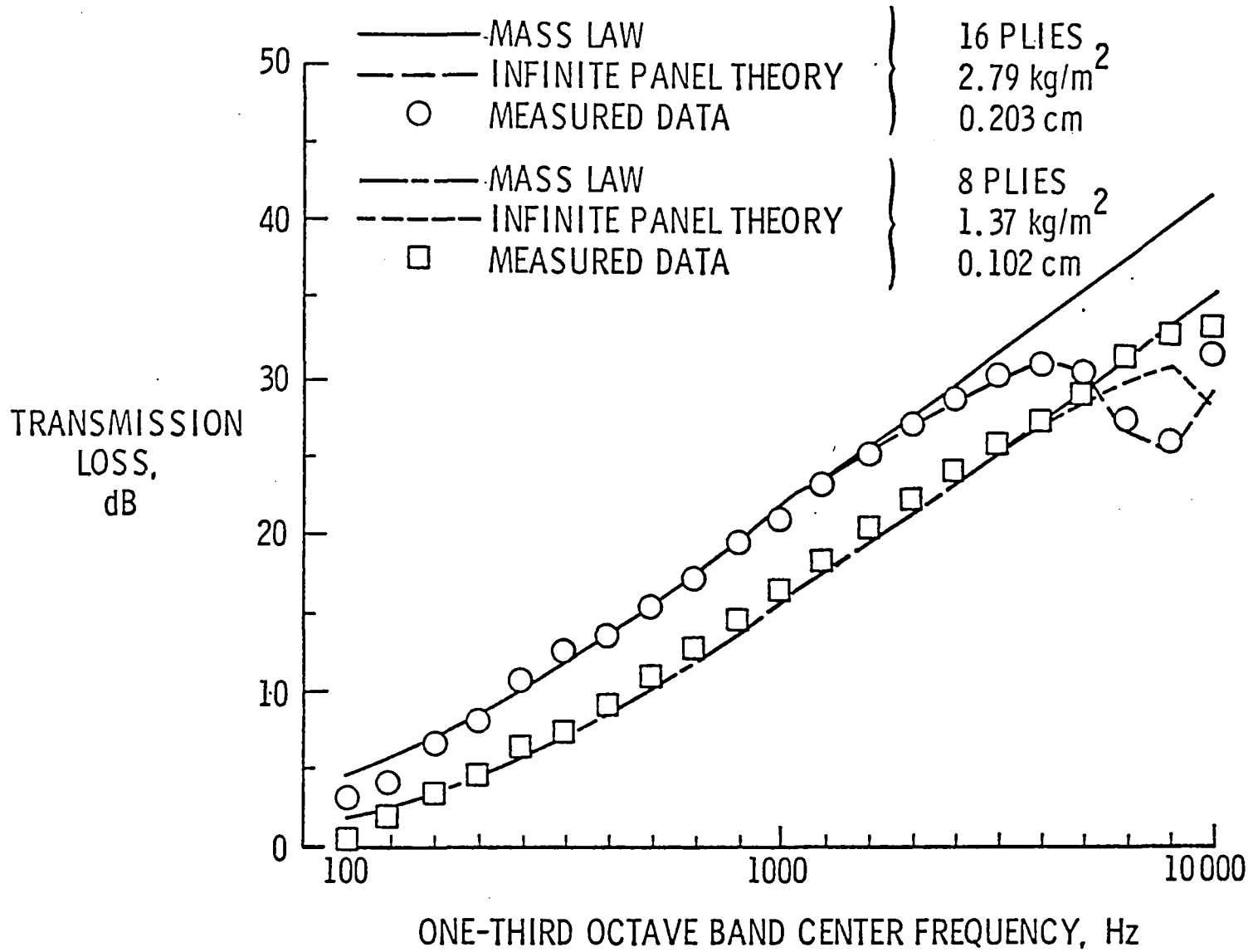


Figure 12.- Noise transmission loss for kevlar/epoxy panels.



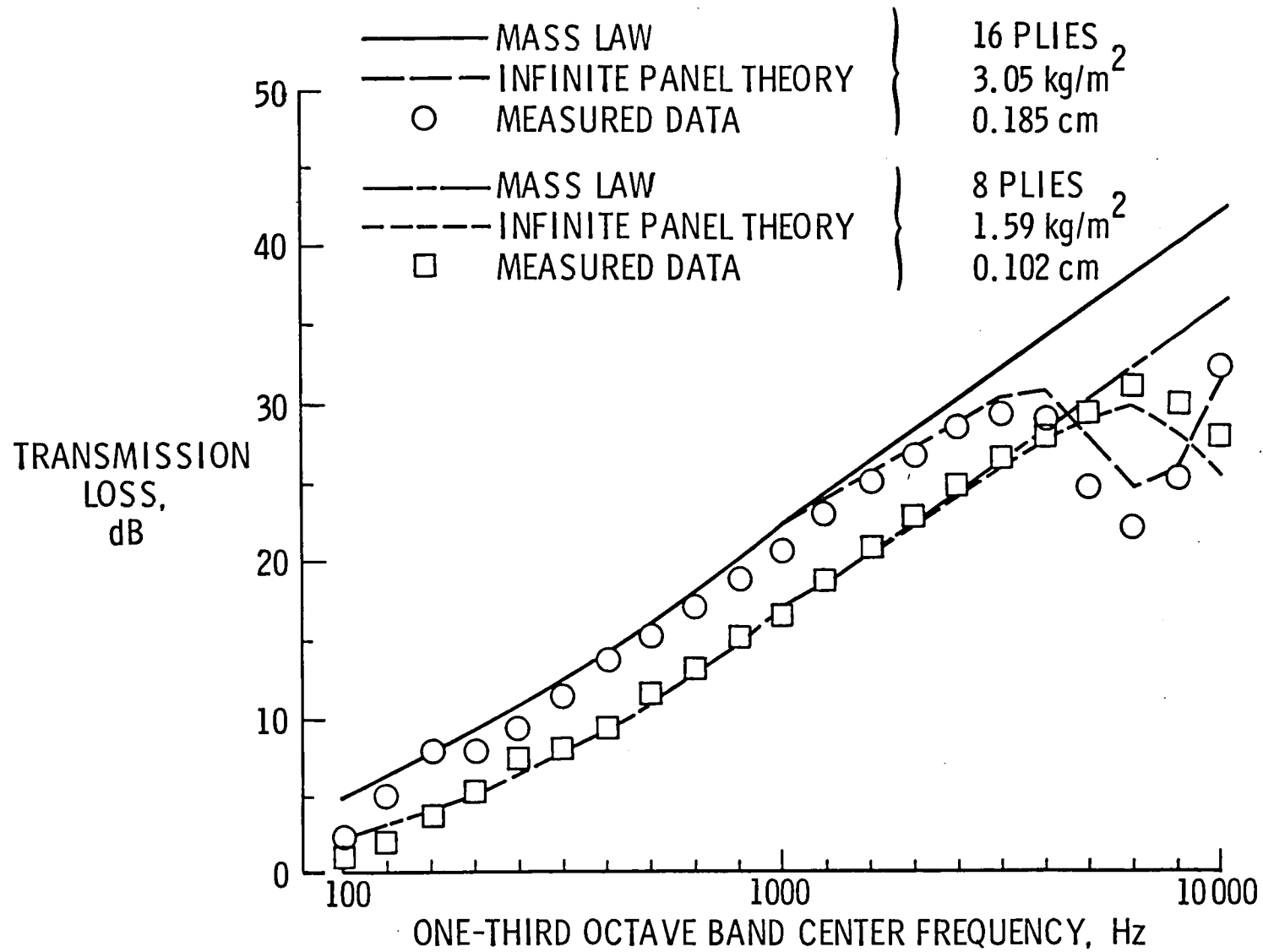


Figure 13.- Noise transmission loss for graphite/epoxy panels.

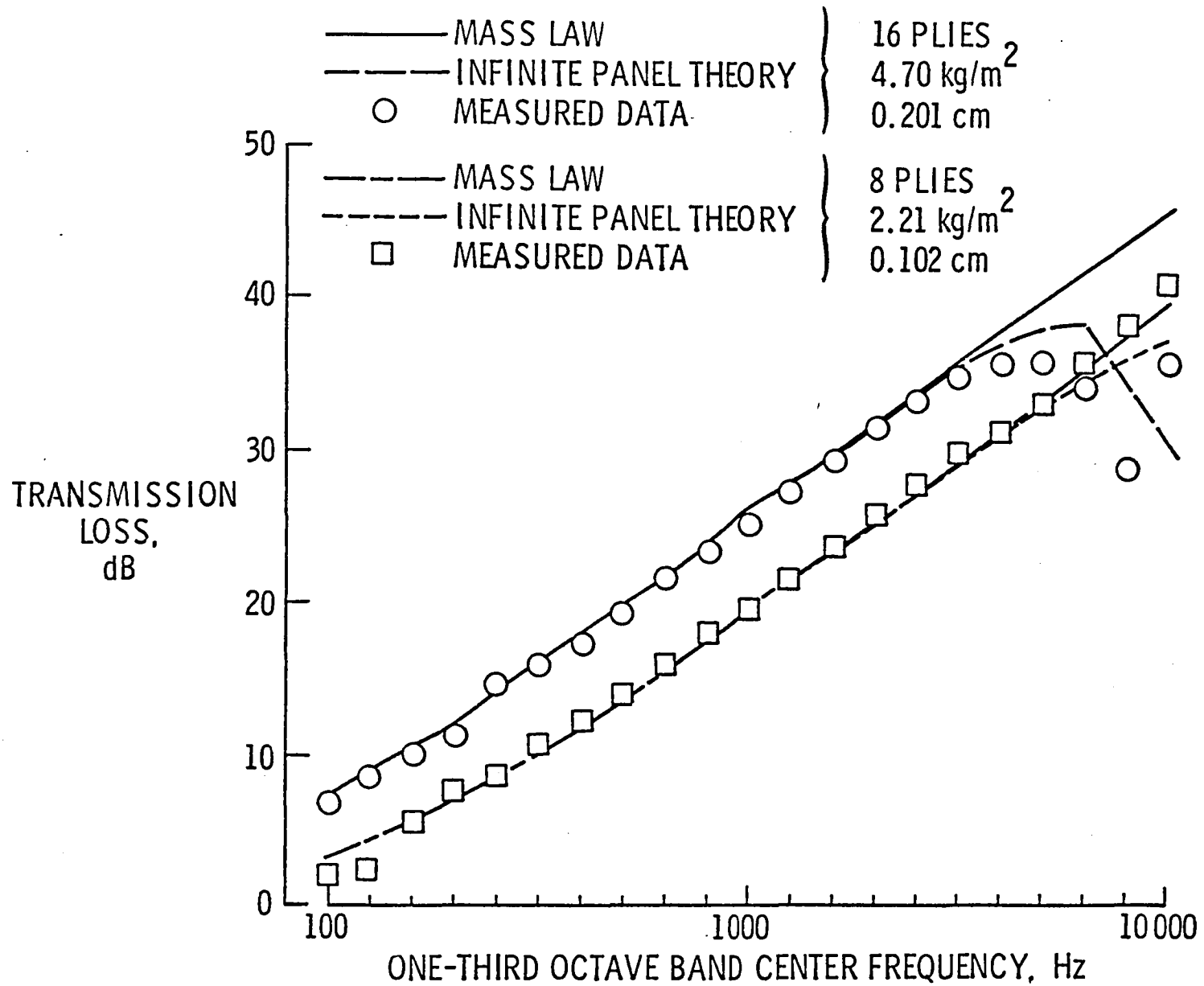
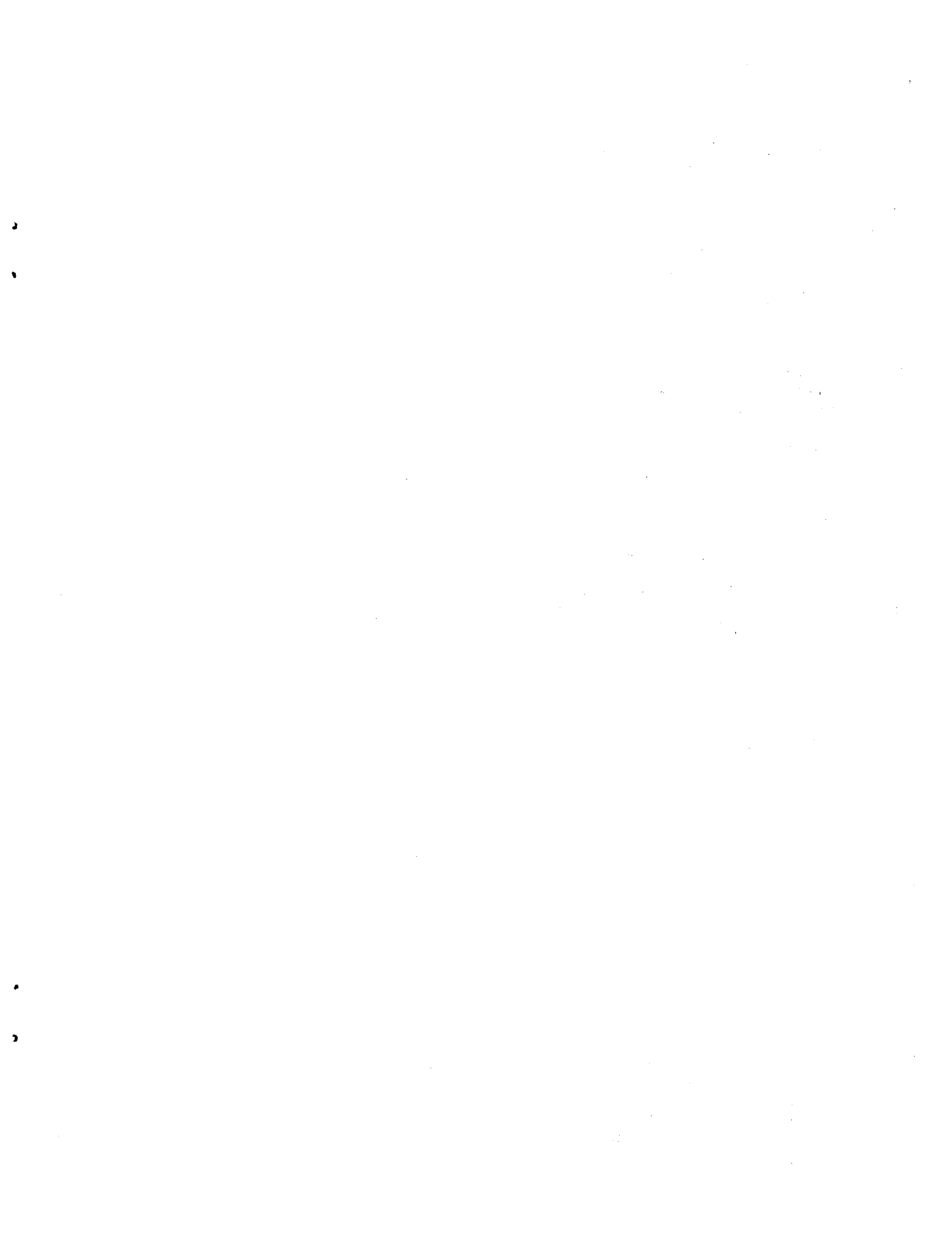


Figure 14.- Noise transmission loss for fiberglass/epoxy panels.



|  |  |                             |  |   |  |
|--|--|-----------------------------|--|---|--|
| 1. Report No.<br>NASA TM-85680   |  | 2. Government Accession No. |  | 3. Recipient's Catalog No.                                    |  |
| 4. Title and Subtitle<br>FIELD-INCIDENCE TRANSMISSION OF TREATED ORTHOTROPIC AND LAMINATED COMPOSITE PANELS  |  |                             |  | 5. Report Date<br>August 1983                                 |  |
|  |  |                             |  | 6. Performing Organization Code<br>532-06-13-02               |  |
| 7. Author(s)<br>Leslie R. Koval  |  |                             |  | 8. Performing Organization Report No.                         |  |
| 9. Performing Organization Name and Address<br>NASA Langley Research Center<br>Hampton, VA 23665   |  |                             |  | 10. Work Unit No.   |  |
|  |  |                             |  | 11. Contract or Grant No.                                     |  |
| 12. Sponsoring Agency Name and Address<br>National Aeronautics and Space Administration<br>Washington, DC 20546  |  |                             |  | 13. Type of Report and Period Covered<br>Technical Memorandum |  |
|  |  |                             |  | 14. Sponsoring Agency Code                                    |  |
| 15. Supplementary Notes<br>Work was performed while employed by NASA Langley Research Center under the ASEE Program.   |  |                             |  |   |  |
| 16. Abstract<br>In an effort to improve understanding of the phenomenon of noise transmission through the sidewalls of an aircraft fuselage, an analytical model has been developed for the field-incidence transmission loss of an orthotropic or laminated composite infinite panel with layers of various noise insulation treatments. The model allows for four types of treatments, impervious limp septa, orthotropic trim panels, porous blankets, and air spaces, while it also takes into account the effects of forward speed.<br><br>Agreement between the model and transmission loss data for treated panels is seen to be fairly good overall. In comparison with transmission loss data for untreated composite panels, excellent agreement occurred. |  |                             |  |   |  |
| 17. Key Words (Suggested by Author(s))<br>Noise transmission<br>Composites<br>Noise insulation treatments<br>Infinite Panel Theory<br>Transmission loss<br>Layered media transmission loss   |  |                             | 18. Distribution Statement<br><br>Unclassified - Unlimited<br><br>Subject category: 71 |   |  |
| 19. Security Classif. (of this report)<br>Unclassified   | 20. Security Classif. (of this page)<br>Unclassified | 21. No. of Pages<br>49      | 22. Price*<br>A03  |   |  |

